PASE: Pro-active Service Embedding in The Mobile Edge

Oleg Kolosov
Computer Science
Technion
Haifa, Israel
kolosov@campus.technion.ac.il

Gala Yadgar
Computer Science
Technion
Haifa, Israel
gala@cs.technion.ac.il

David Breitgand
Hybrid Cloud
IBM Research – Israel
Haifa, Israel
davidbr@il.ibm.com

Dean H. Lorenz
Hybrid Cloud
IBM Research – Israel
Haifa, Israel
dean@il.ibm.com

***Abstract*—Mobile edge computing offers ultra-low latency, high bandwidth, and high reliability. Thus, it can support a plethora of emerging services that can be placed in close proximity to the user. One of the fundamental problems in this context is maximizing the benefit from the placement of networked services, while meeting bandwidth and latency constraints.**

In this study, we propose an adaptive and predictive resource allocation strategy for virtual-network function placement comprising services at the mobile edge. Our study focuses on maximizing the service provider's benefit under user mobility, i.e., uncertainty. This problem is NP-hard, and thus we propose a heuristic solution: we exploit local knowledge about the likely movements of users to speculatively allocate service functions. We allow the service functions to be allocated at different edge nodes, as long as latency and bandwidth constraints are met. We evaluate our proposal against a theoretically optimal algorithm as well as against recent previous work, using widely used simulation tools. We demonstrate that under realistic scenarios, an adaptive and proactive strategy coupled with flexible placement can achieve close-to-optimal benefit.

I. Introduction

Edge computing is a new paradigm for distributed computing, whose premise is to bring computation and data storage closer to the applications. In its broadest sense, the edge is a collection of interoperating micro-datacenters located one or two network hops from the end user. The service provided by the edge architecture is thus adapted to the system topology and the user location. Its advantages— compared to cloud-based services—include shorter response times, lower bandwidth requirements, availability even when temporarily disconnected from the central cloud, and potential improvement in privacy by processing the data locally [1]. Presently, edge computing encompasses an extremely diverse range of technologies, from a plethora of IoT devices to smart city infrastructures, telecommunication 5G/6G multi-access edge computing (MEC), and edge cloud availability zones. The related research challenges and corresponding advances are similarly diverse [2], [3].

In this paper, we focus on networked services in the mobile edge [4]. As stated in the ETSI specification [5], "the MEC system needs to support continuity of the service, mobility of the application, and mobility of application-specific user-related information". To support user mobility, "MEC applications need to run at the right place at the right moment, and might have to move when the conditions evolve". Indeed, the mobile edge opens up new scenarios that transcend device-centric mobile applications and require mobility of low-latency networked services to support, e.g., autonomous vehicles or robotic swarms sharing rich sensor data [6]. We adopt the point-of-view of the edge-service provider, whose goal is to maximize cost-efficiency.

Modern networked services are influenced by recent advancements in network-function virtualization (NFV), software-defined networking (SDN), service-function chaining (SFC), and micro-services-based cloud-native software engineering. Thus, they take the form of virtualized service topologies, where virtual network functions (VNFs) are grouped together into communicating micro-services. Each micro-service defines service-level agreements (SLAs) to its counterparts, where, e.g., its required response time is specified. This model was widely adopted thanks to facilitating large-scale cloud-native deployment and operation and is expected to carry over to the mobile edge. Services are consumed as stateful *service sessions* deployed over a collection of service *functions*.

We consider the following typical business scenario. An edge provider offers virtualized execution environments in the mobile edge, spanning multiple geographic locations. Similarly to the cloud business model, the resources in the mobile edge are offered as-a-service on a pay-as-you-go basis. The users are mobile, e.g., mobile vehicles, making service-session requests from their current locations. Each service session has some duration throughout which it yields benefit to the service provider[1]. If the service is interrupted, i.e., the SLA of the service is violated, then the service provider does not receive benefit during the downtime.

In real commercial systems, this scheme might be somewhat more complex with SLAs being defined in probabilistic terms, allowing some slack for violations without incurring immediate financial repercussions. In this work, we assume

Part of this research work was conducted while the first author was with IBM Research – Israel.

[1]Some services can be provided free of charge to the end users, e.g., by leveraging an advertisement model. We, therefore, refer to a generalized "benefit" for the service owner. The details of how this financial benefit is recovered by the service owner are outside the scope of this paper.

that an operation-support system or a business-support system are responsible for observability, accounting, and billing of both the edge service provider and the service consumers. The provider and consumers will be able to collaboratively detect SLA violations and reconcile these events in the end of the billing period. The details of the involved systems are outside the scope of this work.

The service provider is interested in maximizing its total benefit. To that end, it should balance a tradeoff between the benefit received from the service-session requests and the costs of hosting the services.

The problem of placing service topologies in the edge while maximizing benefit is NP-hard [7]. Optimizing the placement for the mobile edge is at least as complex, due to the uncertainty introduced by user mobility. Fig. 1 demonstrates this complexity: as a user moves with the passage of time, its service (or some of its constituent functions) might be required to migrate to a new location. Such migration is required if the latency constraints can no longer be satisfied by the current placement, given the new location of the user. In a purely *reactive* strategy, the functions of the service will be moved to a new location as a response to the user movement. This strategy is conservative on the hosting expenses, as the resources are allocated only when they are required. However, it might cause a dramatic loss of benefit when user mobility is high. Previous studies [8] showed that *proactive* placement can dramatically reduce downtime by allocating resources at potential future user locations. This potential increase in benefit comes at the cost of increased hosting expenses. This tradeoff was previously addressed by pro-actively allocating resources only in the most expected future user location [9].

In this paper, we propose a novel strategy for pro-active service placement by leveraging fine-grained local predictions of user locations. Inspired by previous work, we consider a slotted time model. In each time slot, we use a forecast that predicts a few most likely locations of each user in the next time slot. We consider the setup cost of proactively transferring the functions' state to these locations, as well as the potential benefit loss due to service session downtime, if the state is transferred reactively. We emphasize that, in this work, we do not focus on the forecast mechanisms *per se*. Instead, we treat forecasting as a pluggable block into the proposed framework and evaluate the sensitivity to forecasting errors.

We evaluate our algorithm, PASE, via simulations against an ideal optimal solution and a state-of-the-art heuristic. We generate realistic user mobility traces using SUMO, an industry-wide recognized open-source vehicle traffic simulator [10], and user-movement traces based on Levy Walk [9], [11], [12], [13]. To compare to the state-of-the-art, we selected recently reported results [9] for a model that is closest to our system model. We demonstrate that PASE is a significantly advantageous strategy under many scenarios of practical importance.

In summary, our contributions are as follows.

- We define a novel framework for service placement in the mobile edge under uncertainty;
- We compare PASE to an optimal offline solution and to the state-of-the-art heuristic, demonstrating its advantage under practical scenarios;
- We thoroughly investigate the tradeoff involved with proactive cost-efficient placement of services in the mobile edge;

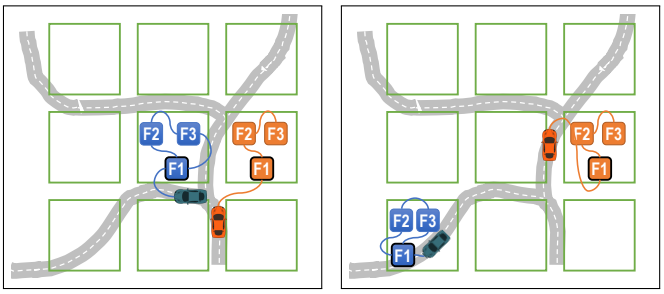

(a) t_n (b) t_{n+1}

Fig. 1. A MEC system with two vehicles, where each square represents the vicinity of a datacenter. The service-function allocations change in response to vehicle movement.

The rest of this paper is organized as follows. In Sec. II, we formally define the service embedding problem and describe our high-level approach. We give the full design and implementation details of PASE in Sec. III. Our evaluation setup and results are described in Sec. IV, with related work surveyed in Sec. V. Sec. VI concludes this work.

II. Problem and Approach

A. Problem description

Below, we define the embedding problem and describe our approach with an outline of our algorithm, PASE. We leave mathematical notations and optimization details to Sec. III.

The proactive service embedding problem: ***Given*** *(a) a substrate network of the mobile edge, (b) a set of service session requests, (c) a forecast of anticipated service sessions;* ***find*** *a feasible embedding of requests onto the substrate network, with maximal benefit.*

The *substrate network* comprises datacenters and links connecting them. Each datacenter has a limited *processing capacity*, that is, available CPU and memory. Each link has limited bandwidth and known latency. The substrate network resources can be consumed in an elastic, pay-as-you-go manner, incurring both *setup* and *usage* costs.

Each *service-session request* is a combination of a service and a user location. Each service session is embedded on the substrate network as a set of interconnected functions, as prescribed by the service topology. Embedding a session on function instances consumes specified request *processing size* on the hosting datacenters and specified BW on the interconnecting links. Processing size is an abstraction of the memory and CPU resources required to process the request. The SLAs for the interacting micro-services are defined through latency constraints between the functions in the topology and between the service and the user. A session embedding is *feasible* if all embedded service functions have enough capacity to process

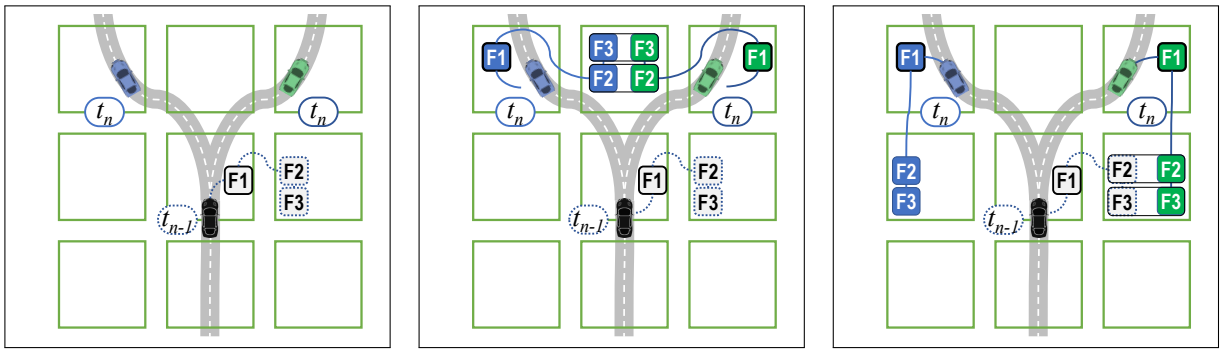

Fig. 2. Proactive allocation based on an existing user location and session embedding (a), and two potential future user locations (b and c).

and can interconnect with each other and with the user at their desired service level; namely, the latency demands are met.

The set of service session requests is dynamic; at each time slot there may be ongoing sessions, new session requests, and sessions that end. Moreover, the user location for an ongoing session may change, possibly requiring modification to its current embedding to ensure it remains feasible.

To allow proactive embedding, a *forecast* of anticipated service sessions is used. At each time slot, based on the current user location, we are provided (as input) with a set of probabilities for this user to be in alternative locations in the next time slot. The user's service session request will be updated according to the new location.

This study focuses on utilizing a given forecast to improve the embedding. The process of deriving predicted user locations from current locations is orthogonal to our algorithm. It might be based on their speed and direction, mobility histories, planned trip, etc. [14], [15], [16]. More advanced methods are available, but this is outside the scope of this work. In our evaluation (Sec. IV), we use a basic analysis of each user's history to derive their next location.

The optimization goal of the proactive service-embedding problem is to maximize overall *provider benefit*. For each service session request, the service provider accrues a benefit for every time slot in which the session is feasibly embedded. The full benefit can only be achieved in a given time slot if the entire service topology is already allocated and set up *before* the time slot starts. For example, an ongoing service session, in which the user can still be served from its current location would accrue full benefit. If the topology is not set up in advance, it can be set up at the beginning of the time slot, which will incur service downtime. In this case, the benefit is reduced (penalized) for any service downtime. For example, new session requests that require new embedding and ongoing sessions that must be re-embedded to accommodate user mobility may accrue only partial benefit. Finally, there is a *setup cost* associated with each new function instantiation. The overall provider benefit is the sum of the full and partial session benefits over all time slots minus the sum of all setup costs.

B. Our approach to proactive allocation

In this section, we describe our main approach to increasing the provider's benefit through proactive allocation. At each time slot, we utilize the session forecast to proactively set up virtual function instances where we anticipate they will be needed at the next time slot. If the forecast is correct then for every service session that utilized these instances, we accrue its full benefit.

There is an overall *late allocation penalty* associated with receiving only partial benefit from sessions that cannot utilize any of the instantiated functions. On the other hand, there is *wasted resources cost* associated with the setup of unused anticipated instances. Maximizing the overall provider benefit requires addressing the tradeoff between this late allocation penalty and the wasted resources cost. Note that this tradeoff is affected by the probability associated with each location as well as the accuracy of the forecast.

As an example, consider the scenario depicted in Fig. 2a. A user (black car) that is at a given position at time t_{n-1} may be located at multiple positions at time t_n. The two possible locations for time t_n are shown in blue (left) and green (right) at the top of Fig. 2a. At its current position, there is an allocation for the requested service session, with three functions split across two datacenters. In this example the latency constraints require that F_1 must be collocated with the user, F_2 must be no further than the neighboring datacenter, and F_2 and F_3 must collocate with each other. The current embedding (as shown in Fig. 2a) reflects the outcome of optimization at the previous time slot.

A proactive embedding solution must consider the two possibilities for the location of the user at time t_n. In order to reduce downtime and maximize the benefit, the service functions should be instantiated at feasible locations. If setup costs are low, then the best proactive strategy is to allocate multiple copies of these functions, covering all the anticipated locations of the user.

Figs. 2b and 2c show two alternatives for feasible embeddings that meet the desired latency constraints for *both* anticipated user locations. The optimization considers the

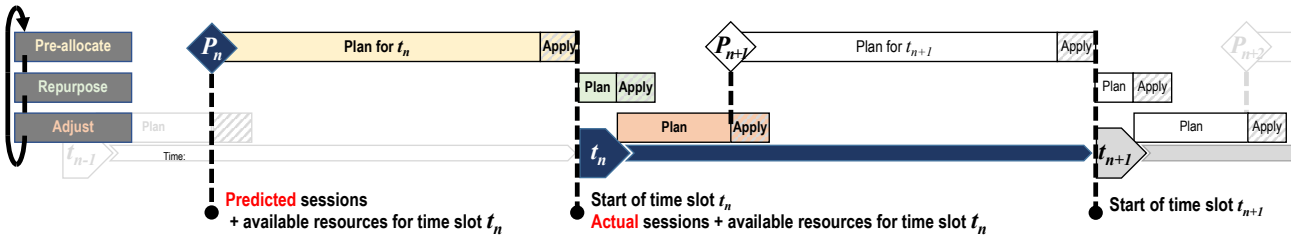

Fig. 3. Timeline of PASE steps and the input used for planning in each step.

available capacity at each datacenter as well as the cost of setting up new function instances.

The capacity calculation considers multiple possibilities for each function. However, the user will eventually be in only one location (either blue or green). Therefore, each function should be set up only once at each datacenter. For example, in Fig. 2b F_2 and F_3 are counted once for both possible user locations, while F_1 is counted twice. Thus, the overall capacity requirements for the proactive allocation shown in Fig. 2b is four shares (assuming all functions require 1 share each). An alternative proactive allocation shown in Fig. 2c requires six capacity shares for t_n.

The setup cost calculation considers the existing embedding (at time t_{n-1}) counting only new instances. For example, in Fig. 2c the existing embedding of F_2 and F_3 are reused, therefore only F_1 is new for the green alternatives and the overall setup cost is 4 new instances. In Fig. 2b the existing embedding is not used; however, both alternatives can utilize the same instances for F_2 and F_3. Therefore, the overall setup cost, in this case, is also 4 new instances.

C. PASE algorithm

We now describe PASE, our algorithm for proactive embedding. The technical details are provided in the next section.

PASE employs a slotted approach, where resources are (re-) allocated at each time slot. At the beginning of each time slot, PASE receives a set of service session requests and the state of the system's resources (the current allocation). The resource allocation for time slot t_n is composed of three partially interleaving optimization steps, which we term *pre-allocation*, *repurposing*, and *adjustment*. Each step has two phases. The *planning phase* receives a precise or approximate view of the system's resources and session requests and generates an embedding plan. The *application phase* applies the plan by instantiating and/or reusing function instances on the substrate datacenters. The different steps differ in their inputs, in the time allocated for their planning phases, and in the logic they use for planning. Fig. 3 depicts the scheduling of these steps and the input each of them receives.

The *pre-allocation* step for time slot t_n takes place during time slot t_{n-1}. Its planning phase is the longest—it optimizes based on a forecast of requests and must consider the inherent uncertainty. Its input is the resource state during time slot t_{n-1} and a prediction of the user locations during time slot t_n. Its application phase sets up new function instances.

The *repurposing step* occurs at the beginning of time slot t_n, when the precise user locations and service session requests are known. It performs an assignment of session requests using functions that are already instantiated. These include ongoing sessions that can keep using their existing functions, as well as new or modified sessions that utilize new instances created in the pre-allocation step. Both the planning and application phases of this step are short. The optimization validates that the latency requirements are met for any interaction between the current user location and the location of the first function. We use a greedy algorithm in order of benefit.

The *adjustment step* attempts to embed any remaining service session requests that were not allocated in the repurposing step. This mostly includes service session requests at time slot t_n that were not anticipated by the forecast at time t_{n-1}. The planning phase of the adjustment step runs the same optimization as that of the pre-allocation step, but rather than using anticipated user locations, the actual locations are used. It also considers only the residual datacenter capacity, ignoring already-allocated resources. Requests embedded at this step experience downtime until the completion of the application phase. Therefore, the run-time constraints for its planning are much more stringent.

For both the pre-allocation and adjustment steps we use the same integer linear program (ILP) formulation (a formal definition is given in Section III-B). We describe the system's resources, the service session requests, and latency requirements as a set of linear constraints and set benefit maximization as the optimization goal. The solution to the ILP provides optimal pre-allocation and adjustment. In our current implementation, we use a commercially-available ILP solver to find a solution to the ILP.

III. ILP Optimization

In this section, we provide an ILP-based optimization for the planning phases of the pre-allocation and adjustment steps of PASE (see Sec. II-C).

A. Notations

The mobile edge substrate is a graph $G(\mathcal{D}, \mathcal{L})$ with a set of datacenters $\mathcal{D}$ and a set of interconnecting links $\mathcal{L}$. C_d denotes the processing capacity of datacenter $d \in \mathcal{D}$; B_ℓ and T_ℓ denote the bandwidth and delay of link $\ell \in \mathcal{L}$, respectively. x_d is the setup cost for instantiating a function on d.

$\mathcal{F}$ and $\mathcal{S}$ denote the sets of available functions and services, respectively. The service topology of each service $s \in \mathcal{S}$ is a

TABLE I
NOTATIONS

sub-strate	$\mathcal{D}$	Set of data centers	$\mathcal{L}$	Set of physical links
	C_d	Capacity of datacenter d	T_ℓ	Physical delay of link ℓ
	x_d	Setup overhead of d	B_ℓ	Bandwidth of link ℓ
services	$\mathcal{F}$	Set of available functions	π_s	Function pairs (links) in s
	Φ_f	Processing size of f	Γ_π	Max delay for $\pi \in \pi_s$
	$\mathcal{S}$	Set of available services	w_π	BW required for $\pi \in \pi_s$
requests	$\mathcal{R}$	Set of requests	$\beta^{\hat{r}}$	Weighted benefit of $\hat{r}$
	β^r	Benefit from $r \in \mathcal{R}$		($\beta^{\hat{r}} \equiv \mathbb{P}(\hat{r})\,\beta^r$)
decision variables	$\delta^r_{d,f}$	'1' iff f is embedded in datacenter d for request r	$y^r_{\pi,\ell}$	'1' iff π is embedded on link ℓ for request r
helper variables	$S^{\hat{r}}$	'1' iff $\hat{r}$ is embedded and is feasible	$e^r_{d,f}$	'1' iff f needs setup on d (previous step embedding)

graph $G^s(\mathcal{F}_s, \pi_s)$, where $\mathcal{F}_s \subseteq \mathcal{F}$ denotes the functions used by the service s and π_s denotes the communication between them. Φ_f denotes the processing size of function $f \in \mathcal{F}$; w_π and γ_π denote the bandwidth consumption and the pairwise latency constraint of link $\pi \in \pi_s$, respectively. γ_π reflects the SLA between functions of the micro-service topology.

$\mathcal{R}$ denotes the set of service session requests and $\mathcal{R}(t)$ denotes the sessions that span time slot t. Each request $r \in \mathcal{R}$ is associated with a specific service $s^r \in \mathcal{S}$, a specific user location $d^r \in \mathcal{D}$, and a benefit β^r. We use the shorthand notation $\pi \in r$ to indicate that r requests service s and $\pi \in \pi_s$. For a time slot t and a request $r \in \mathcal{R}(t)$, $d^r(t)$ denotes the user location at time t and $\beta^r(t)$ denotes the portion of the request benefit that may be accrued at t (namely, β^r divided by the number of slots spanned by r). As each PASE planning iteration works in a single time slot, henceforth, we use only $\mathcal{R}(t)$, $r(t)$, $d^r(t)$, and $\beta^r(t)$. Furthermore, we omit the parameter t to simplify the presentation.

As described in Secs. II-B and II-C, at each time slot, the PASE pre-allocation step utilizes the session forecast to proactively set up virtual function instances where it anticipates they will get used at the next time slot. For each service session request $r \in \mathcal{R}$ (all at time slot t), the forecast provides a set of possible user locations $\{d^r_1, d^r_2, \ldots\}$ together with their corresponding probabilities $\{\mathbb{P}(d^r_1), \mathbb{P}(d^r_2), \ldots\}$. The PASE pre-allocation step instantiates multiple copies of functions to support a feasible embedding of s^r for these anticipated locations. To that end, we partition each request r to a set of sub-requests $\{\hat{r}_1, \hat{r}_2, \ldots\}$, each corresponding to a possible user location $\{d^r_1, d^r_2, \ldots\}$. The benefit of each sub-request $\hat{r}$ is set to the expected benefit of its location, namely $\beta^{\hat{r}} \equiv \mathbb{P}(\hat{r})\,\beta^r$. This allows the optimizer to take into account the tradeoff between the expected benefit of a sub-request and its setup cost. For a sub-request $\hat{r}$, we use the shorthand notation $\hat{r} \in r$ to indicate it is a sub-request of r and the notation $\pi \in \hat{r}$ to indicate that $\pi \in r$.

Table I summarizes our notations.

B. Pre-allocation step

Fig. 4 presents a (mixed-) integer linear program (ILP) formulation to find an optimal embedding at the pre-allocation step of PASE. The variable $\delta^r_{d,f} \in \{0,1\}$ indicates whether the function f is instantiated on datacenter d for request r. Similarly, the variable $y^r_{\pi,\ell} \in \{0,1\}$ indicates whether the pair of functions π communicate over substrate link ℓ for request r.

maximize

$$\sum_{r\in\mathcal{R}}\Big(\sum_{\hat{r}\in r}\beta^{\hat{r}}S^{\hat{r}} - \sum_{d\in\mathcal{D}}\sum_{f\in\mathcal{F}}\delta^r_{d,f}e^r_{d,f}x_d\Big) \tag{1a}$$

s.t.

$$\sum_{r\in\mathcal{R}}\sum_{\pi\in\pi^s} y^r_{\pi,\ell}w_\pi \le B_\ell \qquad \forall \ell\in\mathcal{L} \tag{1b}$$

$$\sum_{r\in\mathcal{R}}\sum_{f\in\mathcal{F}} \delta^r_{d,f}\Phi_f \le C_d \qquad \forall d\in\mathcal{D} \tag{1c}$$

$$y^r_{\pi,\ell} \ge y^{\hat{r}}_{\pi,\ell} \qquad \forall r\in\mathcal{R},\forall \hat{r}\in r,\forall\pi\in r,\forall\ell\in\mathcal{L} \tag{1d}$$

$$\delta^r_{d,f} \ge \delta^{\hat{r}}_{d,f} \qquad \forall r\in\mathcal{R},\forall \hat{r}\in r,\forall f\in r,\forall d\in\mathcal{D} \tag{1e}$$

$$y^r_{\pi,\ell} \le \sum_{\hat{r}\in r} y^{\hat{r}}_{\pi,\ell} \qquad \forall r\in\mathcal{R} \tag{1f}$$

$$\delta^r_{d,f} \le \sum_{\hat{r}\in r} \delta^{\hat{r}}_{d,f} \qquad \forall r\in\mathcal{R},\forall f\in r,\forall d\in\mathcal{D} \tag{1g}$$

Fig. 4. ILP formulation

Equation (1a) provides the optimization goal: the expected total provider benefit. The net provider benefit for each request is its expected benefit minus its setup cost. The helper variable $S^{\hat{r}} \in \{0,1\}$ (see details below) indicates whether the sub-request $\hat{r}$ is embedded and is feasible. If so, its expected benefit $\beta^{\hat{r}}$ is added. The variable $e^r_{d,f} \in \{0,1\}$ indicates whether f induces any setup costs on d. At each time slot, it is a *constant* that depends on the value of $\delta^r_{d,f}$ at the previous time slot. If indicated then the datacenter setup cost is subtracted from the total provider benefit. Note that the setup cost is calculated for each request r rather than for each sub-request $\hat{r}$. If two sub-requests (of the same request) require instantiating a function on the same datacenter then only one copy is needed for both.

Equations (1b) and (1c) ensure link and datacenter capacities are not exceeded. For sub-requests of request r, Eq. (1d) ensures each function pair is embedded only once onto a physical link. Equation (1e) ensures the same for functions on datacenters. Finally, Eqs. (1f) and (1g) require that if a request is embedded then at least one of its sub-requests is also embedded.

The helper variable $S^{\hat{r}}$ is set to 1 only if every logical link $(f,g) = \pi \in \hat{r}$ is embedded on some physical link $(d_f, d_g) \in \mathcal{L}$ and its latency constraint is satisfied. The latency for $\pi = (f,g)$ if embedded on the substrate link $\ell = (d_f, d_g)$ is the sum of the routing delay between d_f and d_g, the processing delay of f on d_f, and the processing delay of g on d_g:

$$\Gamma((f,g) \text{ on } (d_f,d_g)) = y^{\hat{r}}_{\pi,\ell}T_\ell + \Phi_f\delta^{\hat{r}}_{d_f,f} + \Phi_g\delta^{\hat{r}}_{d_g,g}$$

Since it is embedded only on one physical link, we can write

$$\Gamma(\pi) = \sum_{\ell=(d_f,d_g)\in\mathcal{L}}\Big(y^{\hat{r}}_{\pi,\ell}T_\ell + \Phi_f\delta^{\hat{r}}_{d_f,f} + \Phi_g\delta^{\hat{r}}_{d_g,g}\Big) \tag{2}$$

Using Eq. (2), We define $S^{\hat{r}}$ as:

$$S^{\hat{r}} = (\sum_{d\in\mathcal{D}} \delta^{\hat{r}}_{d,f} \geq 1) \wedge (\sum_{d\in\mathcal{D}} \delta^{\hat{r}}_{d,g} \geq 1) \\ \wedge (\Gamma(\pi) \leq \Gamma_{f,g}) \qquad \forall \pi=(f,g)\in\hat{r} \quad (3)$$

Eq. (3) is given in shorthand. We linearize it using a simple transformation.[2]

C. Adjustment step

For the adjustment step of PASE, we use the same ILP of Fig. 4 with a few modifications that significantly simplify it. First, only service session requests that are not yet embedded are considered, so $\mathcal{R}$ is a much smaller set. Second, datacenter capacities $\{C_d\}_{d\in\mathcal{D}}$ and the substrate link capacities $\{B_\ell\}_{\ell\in\mathcal{L}}$ are updated to reflect the remaining unallocated resources. Third, at this stage, the precise user locations are known for every request r; therefore, there is exactly one sub-request $\hat{r} \in r$ with probability $\mathbb{P}(\hat{r}) = 1$. Fourth, $\beta^{\hat{r}} < \beta^r$ is the partial benefit of r after the late allocation penalty is applied. Fifth, every allocation at this step incurs the setup cost (otherwise the resources would have been utilized at the repurposing step); therefore, $e^r_{d,f} \equiv 1$ for all functions and for all datacenters. Equations (1d) to (1g) are no longer needed, thus $\hat{r}$ can be replaced with r in Eqs. (2) and (3).

D. Practical considerations

It is well known that ILP does not scale well. To reduce the ILP input size we trim improbable sub-requests. Theoretically, sub-request probabilities can be arbitrarily low. This may also lead to over-allocation at the pre-allocation step, attempting to cover all possible user locations. We heuristically set a threshold p for minimal request probability and remove any sub-request $\hat{r} \in r$ for which $\mathbb{P}(\hat{r}) \leq p$. Note that now the sum of probabilities of all $\hat{r} \in r$ may be less than 1.

While this heuristic "trimming" worked reasonably well for the problem of the size that we experimented with, further increasing the size of the problem requires some changes. In particular, a standard way of dealing with the scalability problem in ILP is to relax it to become a linear program (LP). LP is highly scalable and can be used with rounding techniques to obtain an integer solution. We note that, in this paper, our main focus was not dealing with the scale of the problem. Rather, our goal was a framework for dealing with intrinsic tradeoffs between reactive and proactive strategies for service embedding into the mobile edge. The ILP building block can be replaced by LP rounding (or other optimization techniques) in future implementations.

IV. Evaluation

We designed our experimental comparative evaluation to answer three questions: (1) how does PASE compare to the most relevant existing policy? (2) how does PASE compare to the theoretically optimal allocation? and, (3) how is PASE affected by the system parameters and user behavior?

[2] $S^{\hat{r}}$ is linearized using $Z = X \wedge Y \rightarrow Z \leq X, Z \leq Y, Z \geq X + Y - 1$ [17].

In the following, we describe the algorithms used in our evaluation (Sec. IV-A), our methodology for generating traces for mobile user service requests (Sec. IV-B), and the parameters of our mobile edge system and service portfolio (Sec. IV-C). We conclude this section by presenting our results and discussing their significance (Sec. IV-D).

A. Algorithms used for comparative study

A survey of related works (see Sec. V) reveals a diverse set of system models and optimization goals, which makes it challenging to directly compare PASE to every existing policy. Therefore, we use the following three algorithms that are most helpful in understanding the value of PASE and intrinsic tradeoffs involved with its performance.

- **MAMI** is presented in [9] for mobility-aware multi-instance function placement. This recent work combines the benefits of proactive and reactive allocation approaches and its model and optimization goal are closest to the ones of PASE. The MAMI algorithm aims at minimizing service session downtime of mobile users by placing services in the mobile edge, such that the service can be consumed with appropriate latency from the expected user locations. MAMI prepares the allocation for each user prior to their arrival in the system. The algorithm allocates one *static* copy of a service in the most probable user location where probability is calculated *a priori* from a long-term history of the user. For the remaining possible locations not covered by the static allocation, MAMI prepares *dynamic* allocations, which do not reserve resources in the datacenters. Upon user arrival to such a location, the dynamic allocation is "activated" if resources are available in the datacenter. "Activation" is made by launching the required functions. The allocation is performed greedily for each user. MAMI places the first function in the datacenter with the highest probability of the user being in its vicinity, and allocates the remaining functions in the service in nearby locations, following capacity and delay constraints.
- **Reactive** is a purely reactive strategy that places user session requests in each time slot according to the actual location of users consuming the sessions. We implement Reactive by limiting PASE to executing the adjustment step only.
- **OPT** is an ideal optimal policy that, prior to the start of every time slot, receives as input the precise user locations. In other words, it has accurate information about where each request will be consumed. We implement OPT by allowing the adjustment step of PASE to execute without a time limit. In practice, the algorithm attains the optimal value within several minutes. For the evaluation, we use this optimal allocation in our simulation as if it were obtained at the start of the time slot, with its input.

All algorithms are implemented in Java. The implementations use IBM CPLEX 22.1 [18] to solve the ILP instances. CPLEX has a probabilistic component, and thus, in our experiment, the performance of PASE is an average of three separate executions with different random seeds. CPLEX runs on Ubuntu 18.04 server equipped with Intel Xeon Platinum

TABLE II
MOBILE EDGE AND SERVICES PORTFOLIO PARAMETERS

Parameter	Value	Parameter	Value
Grid dimensions	4x4	Link capacity [functions]	200
$\|\mathcal{D}\|$, # of datacenters	16	datacenter capacity[PU]	334-2672
Link delay [TU]	6	$\|\mathcal{S}\|$, Service portfolio size	10
Mean service size [# of functions]	3	Mean function pairwise request delay	10
$\|\mathcal{F}\|$, functions portfolio size	10	Mean function size [PU]	2
Avg. # of requests	550	Mean request benefit	200
Function setup cost	10	Late allocation penalty	20%
Sub-request threshold p	5%		

8176 CPU running at 2.1 GHz and 256GB of RAM. The solver uses up to 32 threads. The allotted time limits are 49 seconds for solving the pre-allocation ILP, one second for repurposing in PASE, and 10 seconds for solving the adjustment ILP.

B. Data used for comparative study

Obtaining and generating representative workloads for edge systems is challenging due to their limited deployment which is mostly experimental [19]. Thus, we use an industry-standard open-source traffic simulator, SUMO (Simulator of Urban MObility) [10]. To demonstrate the value of our approach, we extracted a $3.2km \times 3.2km$ section of New York City from OpenStreetMap (OSM) [20] and divided it into a 4x4 grid with cells of equal size. The chosen grid size reflects the locality property evident from the SUMO simulation and the fact a mobile user can only move to an adjacent datacenter during a single time slot. We then use SUMO's OSMWebWizard [21] to generate vehicular traffic of approximately 550 simultaneously active users, with arrival and departure rates of approximately 80 users per minute. We track each user's location during a SUMO execution of 60 minutes, which we split into 60 1-minute time slots. For each slot, service session requests are drawn for each user using Zipf distribution to simulate a typical scenario where a few services are much more popular than others, which are forming a heavy tail of the distribution. Request distributions have been shown to follow the power law and are commonly modeled by Zipf law [22], [23], [24].

We use a separate 60-minute execution of SUMO to collect mobility statistics of users to obtain location predictions for each datacenter. Namely, for each datacenter and its neighbors, we calculate the probability that a user located in this datacenter's cell at time slot t_{n-1} will be located at a neighboring cell at time slot t_n. These probabilities comprise the location predictions used in the PASE pre-allocation step.

To evaluate the sensitivity of PASE to user mobility patterns and to ensure a fair comparison with MAMI, we use an additional mobility model, *Levy Walk* [13], which was used for evaluating MAMI in [9].

Levy walk models long presence at several locations while traveling large distances with unexpected direction changes between locations. Such mobility patterns can characterize taxis, delivery trucks, and other vehicular mobility patterns [11], [12]. We generate requests following the *Improved Levy Walk* defined by Wei et al. in [9]—a Levy walk with a light tail distribution. Following the methodology used in [9], we set a mean pause time of 15 minutes, a maximal travel distance of 3.2km (consistent with the grid dimensions), and use an average speed of 60 km/h. User attrition and turnover rates were set to 15% in each interval, similar to the rates typically used as default parameter values in SUMO simulation.

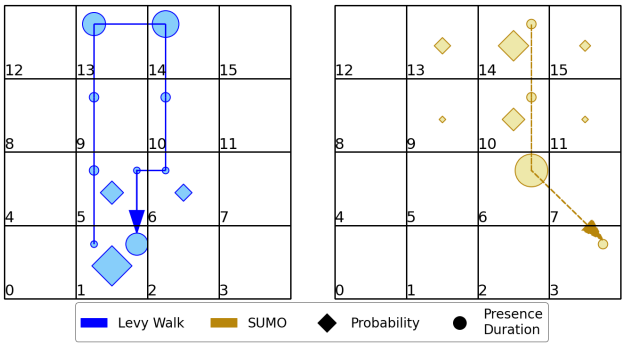

Fig. 5. Mobility of two users under Levy Walk (blue, left) and SUMO (dashed orange, right). Arrows represent path direction. Numbers represent datacenter ID. Circle size indicates the relative time spent in each datacenter and diamond size indicates mobility probabilities from each user's initial location.

We generate location prediction similarly to what is done in [9]: we normalize the time each user spent in each datacenter's cell by its total time in the system, and the resulting ratio is this user's probability to be located in the datacenter, independent of the specific time slot or current location, which means that the user movement is a Markovian process.

Fig. 5 illustrates the difference between the vehicular traffic generated by SUMO and an Improved Levy Walk, showing the path of a representative user generated by each model.

The vehicular paths generated by SUMO (dashed orange) are point-to-point in nature, with users traveling directly between two grid cells. The user in the figure lingered near datacenter 6, and passed through the other cells quickly. The path generated by Levy Walk (blue) is circular in nature, with users returning to cells they frequented earlier. This user lingered in three of the seven datacenters in its path.

Fig. 5 also depicts the predicted locations of each user, relative to their initial location (datacenters 1 and 14 for the Levy Walk and SUMO users, respectively). The size of the colored diamonds in each cell represents the probability that the user will be located in this cell in the following time slot.

In both models, the highest probability is for the user to remain in its current location. However, the predictions for the SUMO user include *all* neighboring cells, while for the Levy Walk one they include only those in the direction of this user's "favorite" cells.

C. Mobile edge parameters used in comparative study

Table II lists the mobile edge and the services portfolio parameters. For all our experiments, we consider a mobile edge with 16 datacenters in a 4x4 grid. We use abstract units of benefit, capacity, latency, and cost, to model the characteristics of the various system components. We set link latency between neighboring datacenters to be six *time units (TU)*. The average

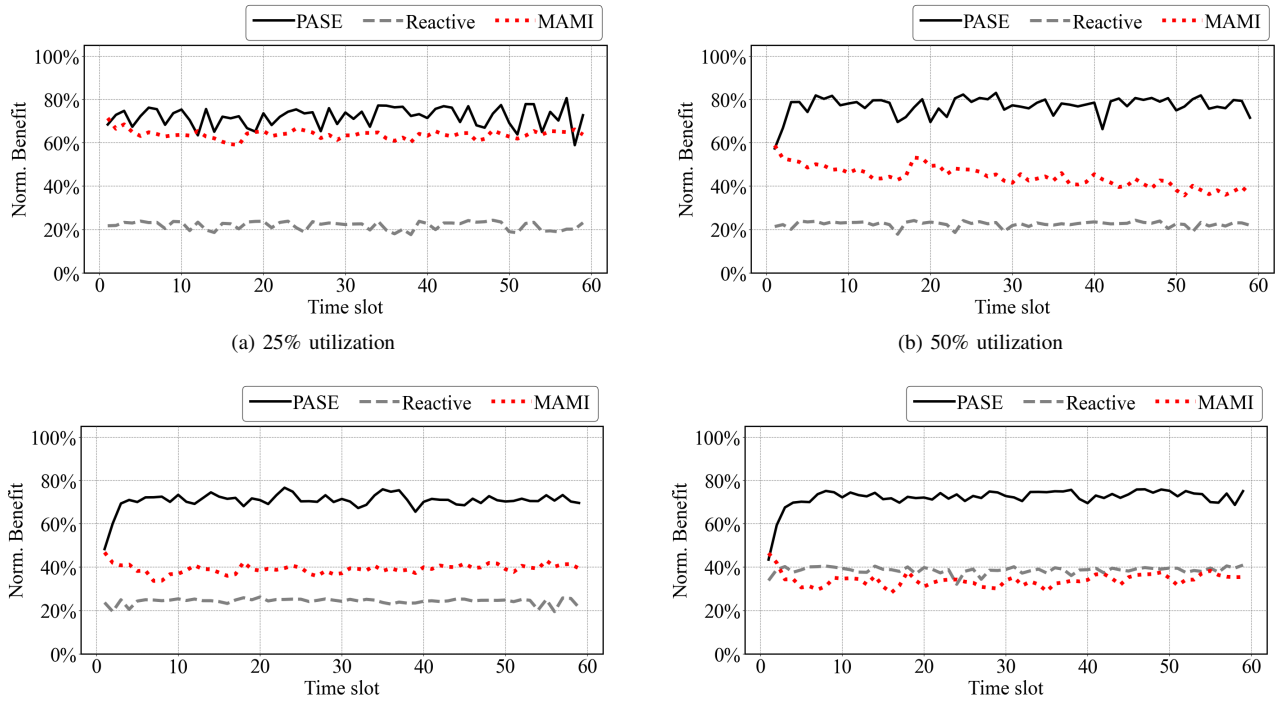

(a) 25% utilization

(b) 50% utilization

(c) 100% utilization

(d) 200% utilization

Fig. 6. The benefit gained by the different policies. Normalized to the benefit of OPT in each time slot. PASE gains the highest benefit, while the benefit of MAMI decreases dramatically as system utilization increases.

delay requirement between each function pair in a service is 10 TU. Similarly to [25], [26], [27], we use Normal distribution to generate the services out of 10 functions, with three functions per service on average. The average capacity requirement of a function is two *processing units (PU)*.

There are approximately 550 users in the system at each time slot. We varied the capacities of the individual datacenters between 334 and 2672 PU, such that the same user workload represents 25%–200% utilization of the system's capacity. The benefit for each request is drawn from a Normal distribution with a mean of 200, and the setup cost of instantiating a function into a new datacenter is 10. The late-allocation penalty for allocation happening in adjustment steps is deducing 20% of the service session request benefit.

D. Experiments

PASE performance. In our first set of experiments, we use mobility traces generated by SUMO. We compare PASE to the strategies described in Sec. IV-A at different levels of *mobile edge utilization*. Utilization is defined as the ratio between the sum of processing units required by all service session requests, and the total processing capacity of all the datacenters in the mobile edge. To neutralize the effect of link capacity bottlenecks, we set unlimited bandwidth for inter-datacenter links.

Fig. 6 shows the benefit gained from each algorithm in each time slot, normalized to the maximum possible benefit in this slot, i.e., to the benefit of OPT. As explained in Sec. II, we consider the benefit from which late-allocation penalty and setup costs were deducted.

When the system utilization is only 25% (Fig. 6a), the benefit of PASE is, on average, 72% of the optimal benefit. The figure shows the value of proactive allocation (the pre-allocation step in PASE) by comparison to Reactive: Reactive gains only approximately 22% of the maximum benefit. The reason is twofold: every successfully embedded function after the time slot's start can only yield reduced benefit due to its late allocation penalty. In addition, Reactive attempts to allocate the functions within much less time than that allocated for PASE in the pre-allocation phase.

In the same setting (25% utilization), MAMI's normalized benefit is 64% on average, only slightly lower than PASE. Indeed, MAMI is designed for underutilized systems, where datacenters have sufficient unallocated capacity to activate dynamic allocations when users arrive in their vicinity. MAMI's benefit is lower than that of PASE because it continues to serve requests with statically allocated services, even when requests with higher potential benefit arrive. PASE, on the other hand, prioritizes the requests that it serves in each time slot to maximize the total benefit of the service provider.

Figs. 6b-6c show how the benefit of the algorithms changes with increasing mobile edge utilization values. In our experiments, higher utilization levels are realized by simulating the same set of service session requests while decreasing the total datacenter capacity. As a result, the absolute benefit gained by OPT decreases as well. However, as one can see in Fig. 6b,

at 50% mobile edge utilization, the normalized benefit of PASE remains the same as for 25%, while that of MAMI dramatically decreases.

Furthermore, as one can clearly observe in Fig. 6d, PASE still manages to attain the same 70% of the normalized benefit even at 200% utilization. The normalized benefit of MAMI, however, decreases dramatically even further, as a result of increased system utilization, to as little as 34%, on average—this is essentially the same benefit as that of Reactive. MAMI's poor behavior at high mobile-edge utilization levels is caused by static allocations that prevent dynamic allocations of functions. At the same time, many static allocations become irrelevant to the users' current locations. Reactive improves at 200% utilization since it still serves a similar number of requests in each interval, while OPT gains approximately 50% less benefit compared to its benefit with 25% utilization.

Fig. 7a shows the absolute value of the total benefit gained in the same experiments. We exclude the first 10 time slots in which the algorithms stabilize. Fig. 7a also shows a breakdown of the benefit gained by each step in the various algorithms. PASE gains approximately 35% of its benefit from functions allocated in the pre-allocation step, and an additional 35% and 30% from the repurposing and adjustment steps, respectively. The high benefit achieved from repurposing can be attributed to the skewness in service popularity: the most popular services are requested by more users at any given location.

As expected, the benefit of Reactive is hardly affected by the system utilization. While it needs to reallocate more functions as utilization grows, the time allocated for its planning step (i.e., solving the ILP instance) does not change and remains at 10 seconds. Even at 50% utilization, the pure Reactive strategy appears not to scale.

The effect of setup cost. To evaluate the effect of the setup cost on PASE, we repeated the experiments at various levels of mobile edge utilization. In this experiment, we fixed the number of functions in each service to three. We show the results for 50% utilization level, having verified the effect is similar in all utilization levels. We varied the setup cost from 20 to 180, which is equivalent to 10%-90% of the mean request benefit. Fig. 8 shows the total absolute benefit of each policy. MAMI is excluded from this experiment because the setup cost is not considered in its model and does not affect its allocation decisions. As expected, the benefit accrued by all policies decreases with the setup cost because the solver more aggressively avoids function migrations that might be necessary to admit high-benefit requests.

The effect of prediction accuracy. We define the *misprediction rate* as the portion of incorrect predictions in the predicted locations. To evaluate the sensitivity of the different policies to prediction accuracy, we repeat the experiments for different levels of the mobile-edge utilization while varying the misprediction rate. Here, too, the effect is similar for all utilization levels, and we present only the results for 50% mobile edge utilization. In each time slot, we modify the predicted locations given as input to the algorithms. For misprediction rate r, $100\% - r$ of the predicted user locations are their precise future locations, and the remaining r are random locations different from their true future locations.

Fig. 9 shows the benefit gained by each policy, normalized to that of OPT. When the predictions are accurate (0% mispredictions), PASE achieves almost 100% of the benefit obtained by OPT, because its pre-allocation step allocates functions according to the true user locations. The benefit of PASE decreases as the misprediction rate increases because the effectiveness of the pre-allocation step decreases. Thanks to repurposing and adjustment steps, PASE manages to recover from a large portion of inaccurate predictions, thus reaching 66% of the benefit of OPT at 100% misprediction rate.

The benefit of MAMI also decreases with the increase in misprediction rate, from a normalized benefit of 61% to 0, with misprediction rates of 0 to 100%, respectively. MAMI is more sensitive to mispredictions than PASE because it is unable to activate its dynamic allocations for users that arrive at unexpected locations. The normalized benefit of Reactive remains low, although it approaches that of MAMI with a misprediction rate of 60%.

The effect of mobility patterns. To evaluate the sensitivity of PASE to user mobility patterns, we repeated the experiments in Fig. 6 and Fig. 7a with user locations derived from the Levy Walk traces. Fig. 7b shows the total benefit gained by each policy in each experiment, with varying levels of mobile edge utilization. The first 10 time slots are excluded as in Fig. 7a. PASE gains higher benefit from the Levy Walk users than the SUMO users thanks to the increased accuracy of the user-specific predicted locations. As a result, 68% of PASE's benefit comes from pre-allocated functions, 33% more than its percentage for the SUMO paths. The benefit of OPT and Reactive is not affected by prediction accuracy.

MAMI's benefit with Levy Walk is considerably higher than with the SUMO-generated traces. Indeed, MAMI was designed for users with predictable locations, and its benefit in the underutilized system is 90% of the maximum. However, this benefit decreases dramatically as mobile edge utilization increases, for the reasons discussed above. This experiment highlights the advantages of PASE, which is less vulnerable to unpredictable user mobility and highly utilized systems.

V. Related Work

Our study focuses on service embedding under uncertainty caused by user mobility. Previous studies addressed many variants of embedding both in the context of SFC embedding and virtual network embedding (VNE) problems in various environments. Typically uncertainty is not in the focus in these setups. For example, embedding in cloud systems [28], [29], [30], [31], [32] does not involve mobile users, thus resolving one of the main reasons for uncertainty.

Our work shares some concepts with previous studies, such as provider-aware optimization [33] and allocation with ILP optimization [34].

Other studies do not address user mobility explicitly. The policies in [27], [35], [36], [37] allocate SFCs under constraints on CPU, memory, bandwidth, latency, and other 5G

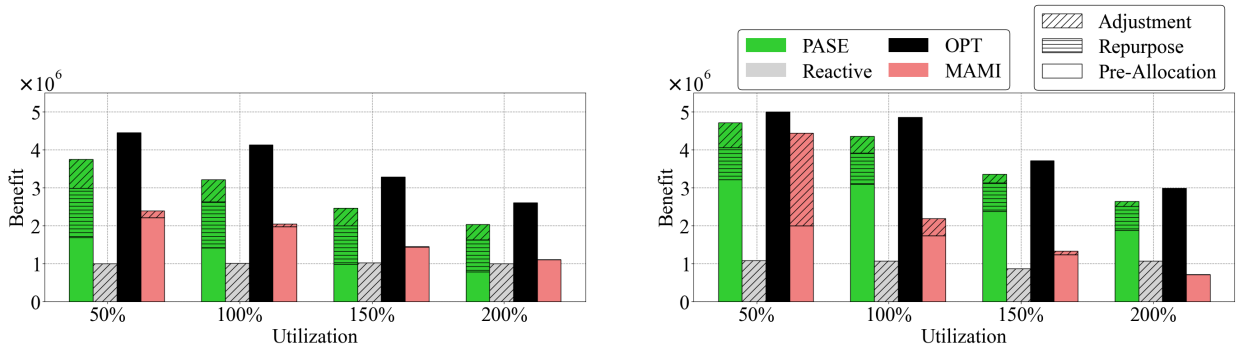

(a) SUMO

(b) Levy Walk

Fig. 7. Breakdown of absolute total benefit for SUMO (a) and Levy Walk (b).

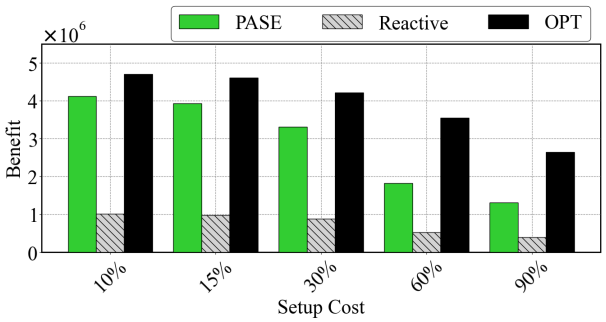

Fig. 8. The effect of the setup cost. As the cost increases, the benefit of both OPT and PASE decreases as they avoid function migration.

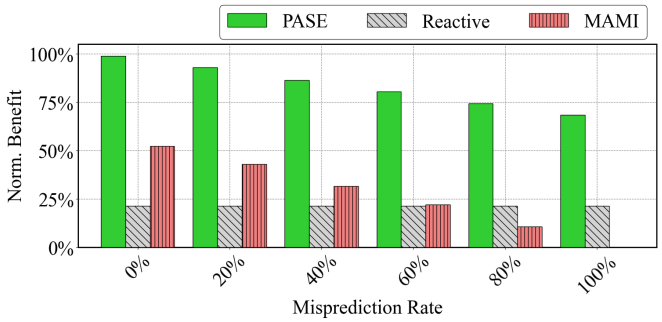

Fig. 9. The benefit of both PASE and MAMI decreases with the number of wrong predictions, but PASE is less vulnerable.

and edge parameters. These studies allocate resources for requests upon arrival, in an online fashion. This approach for addressing uncertainty handles only incoming requests, while the old ones remain unaffected. In contrast, PASE searches for an optimal allocation given all outstanding requests in each time slot.

Embedding approaches involving machine learning are becoming increasingly popular. These studies [38], [39], [40] improve resource allocation by predicting user locations and demand. However, they limit the allocation of application resources to a single location. Predictions generated by machine-learning can be easily incorporated into PASE as input. Different forecast approaches can work in combination with our algorithm, and our results show that the benefit to the provider increases with the quality of the probabilistic input.

Coniglio et al. [41] address virtual network embedding under uncertainty with the goal of maximizing total request revenue. They allocate instances whose constraints are likely to be met. The uncertainty in their model results from an unexpected load, while our model addresses the more specific challenge of uncertainty in user locations. In addition, their approach addresses allocation in a single timeslot, as opposed to the continuous approach of PASE. Coniglio et al. [41] limit embedding of one virtual node onto a physical node, while we have no such limitation to maximize potential revenue.

Wei et al. [9] propose an algorithm based on expected user locations. They reserve resources in advance for more probable scenarios, while dynamically planning allocation for less probable cases. Our approach solves an ILP based on actual conditions in real-time. Also, we require less accurate probabilities than defined in [9]. We discuss the algorithm described in [9] in detail in this work and evaluate it in Sec. V.

Saurez et al. [42] propose a control plane for edge datacenters that allocates services while considering user locations, latency constraints, and available resources. Similar to our approach, they employ proactive and reactive policies. However, their solution does not aim for optimality, and requests are served by order of arrival.

Several works [27], [35], [42] apply a single latency constraint across the entire service, taking an end-to-end approach. In contrast, we apply pairwise latency constraints to reflect the SLAs between functions. Satisfying pairwise constraints guarantees the satisfaction of the overall service SLA.

VI. Conclusions

We presented PASE, an algorithmic framework that exploits local knowledge about expected user movements in the mobile edge. PASE proactively sets up functions of a service session in the most anticipated locations to maximize the service owner benefit while minimizing downtime for the users. Thanks to its proactive strategy and real-time adaptiveness, PASE outperforms the state-of-the-art policy for this model by a considerable margin and is also considerably closer to the theoretical optimum.

One future work direction is to extend our model to encompass graceful QoS degradation due to under-allocation of resources, rather than the all-or-nothing allocation model studied in this work. Another potential direction is to relax the ILP model and develop a fast rounding heuristic to improve the scalability of PASE. Finally, we plan to explore strategies exploiting multi-time slot predictions (e.g., capturing typical daily vehicle routes) at the level of individual users.

ACKNOWLEDGMENT

The research of Oleg Kolosov was supported in part by US-Israel BSF grant 2021613 and by ISF grant 807/20.

REFERENCES

[1] J. Davis, P. Shih, and A. Marcham, "State of the edge 2018: A market and ecosystem report for edge computing," Report, 2018.

[2] Cao, Keyan and Liu, Yefan and Meng, Gongjie and Sun, Qimeng, "An overview on edge computing research," *IEEE Access*, vol. 8, 2020.

[3] Y. Mansouri and M. A. Babar, "A review of edge computing: Features and resource virtualization," *J. of Parallel and Distributed Computing*, vol. 150, pp. 155–183, 2021.

[4] Sami Kekki et.al., "MEC in 5G networks," https://www.etsi.org/images/files/ETSIWhitePapers/etsi_wp28_mec_in_5G_FINAL.pdf, 2018.

[5] ETSI, "ETSI GS MEC 002 V2.1.1 (2018-10), Multi-access edge computing (MEC); Phase 2: use cases and requirements," 2018.

[6] R. A. Addad, D. L. C. Dutra, M. Bagaa, T. Taleb, and H. Flinck, "Towards studying service function chain migration patterns in 5G networks and beyond," in *GLOBECOM*, 2019, pp. 1–6.

[7] A. L. É. Battisti, E. L. C. Macedo, M. I. P. Josué, H. Barbalho, F. C. Delicato, D. C. Muchaluat-Saade, P. F. Pires, D. P. d. Mattos, and A. C. B. d. Oliveira, "A novel strategy for VNF placement in edge computing environments," *Future Internet*, vol. 14, no. 12, p. 361, 2022.

[8] I. Farris, T. Taleb, M. Bagaa, and H. Flick, "Optimizing service replication for mobile delay-sensitive applications in 5g edge network," in *IEEE ICC*. IEEE, 2017, pp. 1–6.

[9] Q. Wei, P. Han, and Y. Liu, "Mobility-aware multi-instance vnf placement in mobile edge computing networks," in *2021 Int. Wireless Communications and Mobile Computing*. IEEE, 2021, pp. 1303–1308.

[10] D. Krajzewicz, J. Erdmann, M. Behrisch, and L. Bieker, "Recent development and applications of SUMO—simulation of urban mobility," *Int. J. on Advances in Systems and Measurements*, vol. 5, no. 3&4, 2012.

[11] Y. Cao, Y. Li, J. Zhou, D. Jin, L. Su, and L. Zeng, "Recognizing the Levy-walk nature of vehicle mobility." in *IWCMC*, 2011, pp. 1194–1199.

[12] Y. Li, Z. Wang, D. Jin, L. Zeng, and S. Chen, "Collaborative vehicular content dissemination with directional antennas," *IEEE Trans. on Wireless Communications*, vol. 11, no. 4, pp. 1301–1306, 2012.

[13] I. Rhee, M. Shin, S. Hong, K. Lee, S. J. Kim, and S. Chong, "On the Levy-walk nature of human mobility," *IEEE/ACM Trans. Netw.*, vol. 19, no. 3, pp. 630–643, 2011.

[14] X. Gong and S. Manoharan, "On predicting vehicle tracks," in *Proc. of 2011 IEEE Pacific Rim Conf. on Communications, Computers and Signal Processing*. IEEE, 2011, pp. 31–36.

[15] W. Zhan, C. Luo, G. Min, C. Wang, Q. Zhu, and H. Duan, "Mobility-aware multi-user offloading optimization for mobile edge computing," *IEEE Trans. Veh. Technol.*, vol. 69, no. 3, pp. 3341–3356, 2020.

[16] C.-L. Wu, T.-C. Chiu, C.-Y. Wang, and A.-C. Pang, "Mobility-aware deep reinforcement learning with glimpse mobility prediction in edge computing," in *IEEE ICC*. IEEE, 2020, pp. 1–7.

[17] M. Asghari, A. M. Fathollahi-Fard, S. M. J. Mirzapour Al-e hashem, and M. A. Dulebenets, "Transformation and linearization techniques in optimization: A state-of-the-art survey," *Mathematics*, vol. 10, no. 2, 2022.

[18] "CPLEX Optimizer," https://www.ibm.com/analytics/cplex-optimizer, accessed: 2023-01-19.

[19] O. Kolosov, G. Yadgar, S. Maheshwari, and E. Soljanin, "Benchmarking in the dark: On the absence of comprehensive edge datasets," in *3rd USENIX Workshop on Hot Topics in Edge Computing*, 2020.

[20] M. Haklay and P. Weber, "Openstreetmap: User-generated street maps," *IEEE Pervasive computing*, vol. 7, no. 4, pp. 12–18, 2008.

[21] "OSMWebWizard," https://sumo.dlr.de/docs/Tutorials/OSMWebWizard.html, 2023 (accessed January 21, 2023).

[22] Y. Nam, S. Song, and J.-M. Chung, "Clustered NFV service chaining optimization in mobile edge clouds," *IEEE Communications Letters*, vol. 21, no. 2, pp. 350–353, 2016.

[23] L. Breslau, P. Cao, L. Fan, G. Phillips, and S. Shenker, "Web caching and Zipf-like distributions: Evidence and implications," in *INFOCOM'99. Eighteenth Annual Joint Conf. of the IEEE Computer and Commun. Societies. Proceed.IEEE*, vol. 1. IEEE, 1999, pp. 126–134.

[24] B. F. Cooper, A. Silberstein, E. Tam, R. Ramakrishnan, and R. Sears, "Benchmarking cloud serving systems with YCSB," in *1st ACM Symp. on Cloud Computing (SoCC)*, 2010.

[25] X. Shang, Y. Huang, Z. Liu, and Y. Yang, "Reducing the service function chain backup cost over the edge and cloud by a self-adapting scheme," *IEEE Trans. on Mobile Computing*, 2021.

[26] X. Huang, S. Bian, X. Gao, W. Wu, Z. Shao, Y. Yang, and J. C. Lui, "Online VNF chaining and predictive scheduling: Optimality and trade-offs," *IEEE/ACM Trans. Netw.*, vol. 29, no. 4, pp. 1867–1880, 2021.

[27] A. Mohamad and H. S. Hassanein, "On demonstrating the gain of SFC placement with VNF sharing at the edge," in *2019 IEEE Global Communications Conf. (GLOBECOM)*. IEEE, 2019, pp. 1–6.

[28] W. Chen, Z. Wang, H. Zhang, X. Yin, and X. Shi, "Cost-efficient dynamic service function chain embedding in edge clouds," in *17th Int. CNSM*. IEEE, 2021, pp. 310–318.

[29] Z. Luo, C. Wu, Z. Li, and W. Zhou, "Scaling geo-distributed network function chains: A prediction and learning framework," *IEEE J. on Selected Areas in Communications*, vol. 37, no. 8, pp. 1838–1850, 2019.

[30] J. Pei, P. Hong, K. Xue, and D. Li, "Efficiently embedding service function chains with dynamic virtual network function placement in geo-distributed cloud system," *IEEE Trans. on Parallel and Distributed Systems*, vol. 30, no. 10, pp. 2179–2192, 2018.

[31] X. Fei, F. Liu, H. Xu, and H. Jin, "Towards load-balanced VNF assignment in geo-distributed NFV infrastructure," in *2017 IEEE/ACM 25th Int. Symp. on Quality of Service (IWQoS)*. IEEE, 2017, pp. 1–10.

[32] M. Mechtri, C. Ghribi, and D. Zeghlache, "A scalable algorithm for the placement of service function chains," *IEEE Trans. on network and service management*, vol. 13, no. 3, pp. 533–546, 2016.

[33] Z. Zhou, Q. Wu, and X. Chen, "Online orchestration of cross-edge service function chaining for cost-efficient edge computing," *IEEE J. Sel. Area. Comm.*, vol. 37, no. 8, pp. 1866–1880, 2019.

[34] D. Bhamare, M. Samaka, A. Erbad, R. Jain, L. Gupta, and H. A. Chan, "Optimal virtual network function placement in multi-cloud service function chaining architecture," *Comput. Commun.*, vol. 102, pp. 1–16, 2017.

[35] P. Jin, X. Fei, Q. Zhang, F. Liu, and B. Li, "Latency-aware VNF chain deployment with efficient resource reuse at network edge," in *IEEE INFOCOM*. IEEE, 2020, pp. 267–276.

[36] S. Agarwal, F. Malandrino, C. F. Chiasserini, and S. De, "VNF placement and resource allocation for the support of vertical services in 5g networks," *IEEE/ACM Trans. Netw.*, vol. 27, no. 1, pp. 433–446, 2019.

[37] T.-W. Kuo, B.-H. Liou, K. C.-J. Lin, and M.-J. Tsai, "Deploying chains of virtual network functions: On the relation between link and server usage," *IEEE/ACM Trans. Netw.*, vol. 26, no. 4, pp. 1562–1576, 2018.

[38] A. Rago, G. Piro, G. Boggia, and P. Dini, "Anticipatory allocation of communication and computational resources at the edge using spatio-temporal dynamics of mobile users," *IEEE Trans. on Network and Service Management*, vol. 18, no. 4, pp. 4548–4562, 2021.

[39] O. Tao, X. Chen, Z. Zhou, L. Li, and X. Tan, "Adaptive user-managed service placement for mobile edge computing via contextual multi-armed bandit learning," *IEEE Trans. on Mobile Computing*, 2021.

[40] T. Wang, Q. Fan, X. Li, X. Zhang, Q. Xiong, S. Fu, and M. Gao, "DRL-SFCP: Adaptive service function chains placement with deep reinforcement learning," in *IEEE ICC*. IEEE, 2021, pp. 1–6.

[41] S. Coniglio, A. M. Koster, and M. Tieves, "Virtual network embedding under uncertainty: Exact and heuristic approaches," in *2015 11th Int. DRCN*. IEEE, 2015, pp. 1–8.

[42] E. Saurez, H. Gupta, A. Daglis, and U. Ramachandran, "OneEdge: An efficient control plane for geo-distributed infrastructures," in *Proc. of the ACM Symp. on Cloud Computing*, 2021, pp. 182–196.